A STUDY OF EARTHQUAKE PREDICTION AND THE TECTONICS OF THE NORTHEASTERN CARIBBEAN: A CONTINUING EXPERIMENT IN TWO MAJOR SEISMIC GAPS

W. R. McCann, A. L. Kafka, and L. R. Sykes

Lamont-Doherty Geological Observatory of Columbia University
Palisades, New York 10964

USGS CONTRACT NO. 14-08-0001-16748
Supported by the EARTHQUAKE HAZARDS REDUCTION PROGRAM

OPEN-FILE NO. 81-884

U.S. Geological Survey
OPEN FILE REPORT

TECHNICAL STATUS OF SEISMIC NETWORK

During the period November 1977 through October 1980 Lamont-Geological Observatory continued to operate a network of 17 seismograph stations in the northeastern Caribbean (Figure 1a,b; Table 1). Throughout this period several significant improvements to the detection and recording equipment were implemented.

In March 1979 a Digital Recording System (DRS) with an event-trigger was installed at the central recording site on St. Thomas, and this system has operated without failure since then. The DRS has an analog trigger system. Six of the network stations are trigger stations, any pair of which can cause the system to initiate recording. The DRS presently records 32 channels of information from the 17 stations. Upon triggering, the DRS dumps 25 seconds of pre-event memory onto magnetic tape, records the event and, continues recording until 20 seconds after the system sees the last 2 triggers. Each channel records information at a rate of 100 samples per second and has a dynamic range of 72 db. As the dynamic range of the telemetry links is about 46 to 52 db, the DRS does not limit the information gathered. Electrical power comes from the local power authority with an uninterruptable power supply and battery bank serving as a backup system.

Several changes in the configuration of the network occurred during the last three years. In March 1979 a two component station was installed on Virgin Gorda. This station operates at high gain and has helped offset the problem of having a noisy station on the geographically strategic island of Anegada. In December 1979 two new

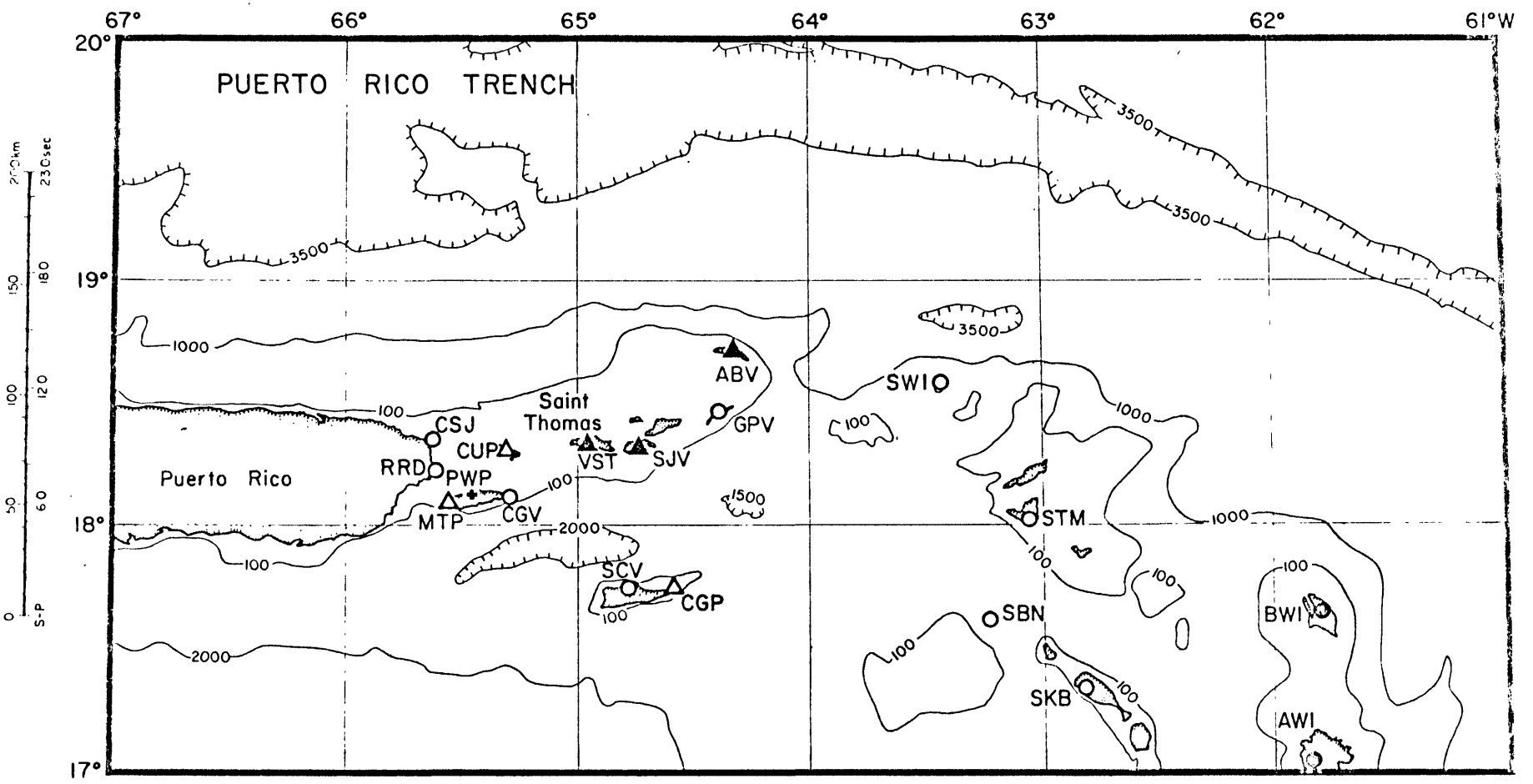

Figure 1a: Present configuration of the northeastern Caribbean seismic network including sites of strong motion instruments. Signals are telemetered to St. Thomas where they are recorded on a digital recording system. Symbols are as follows: circles - single component stations; triangles - three component stations; cross- closed stations; solid symbols - SMA site.

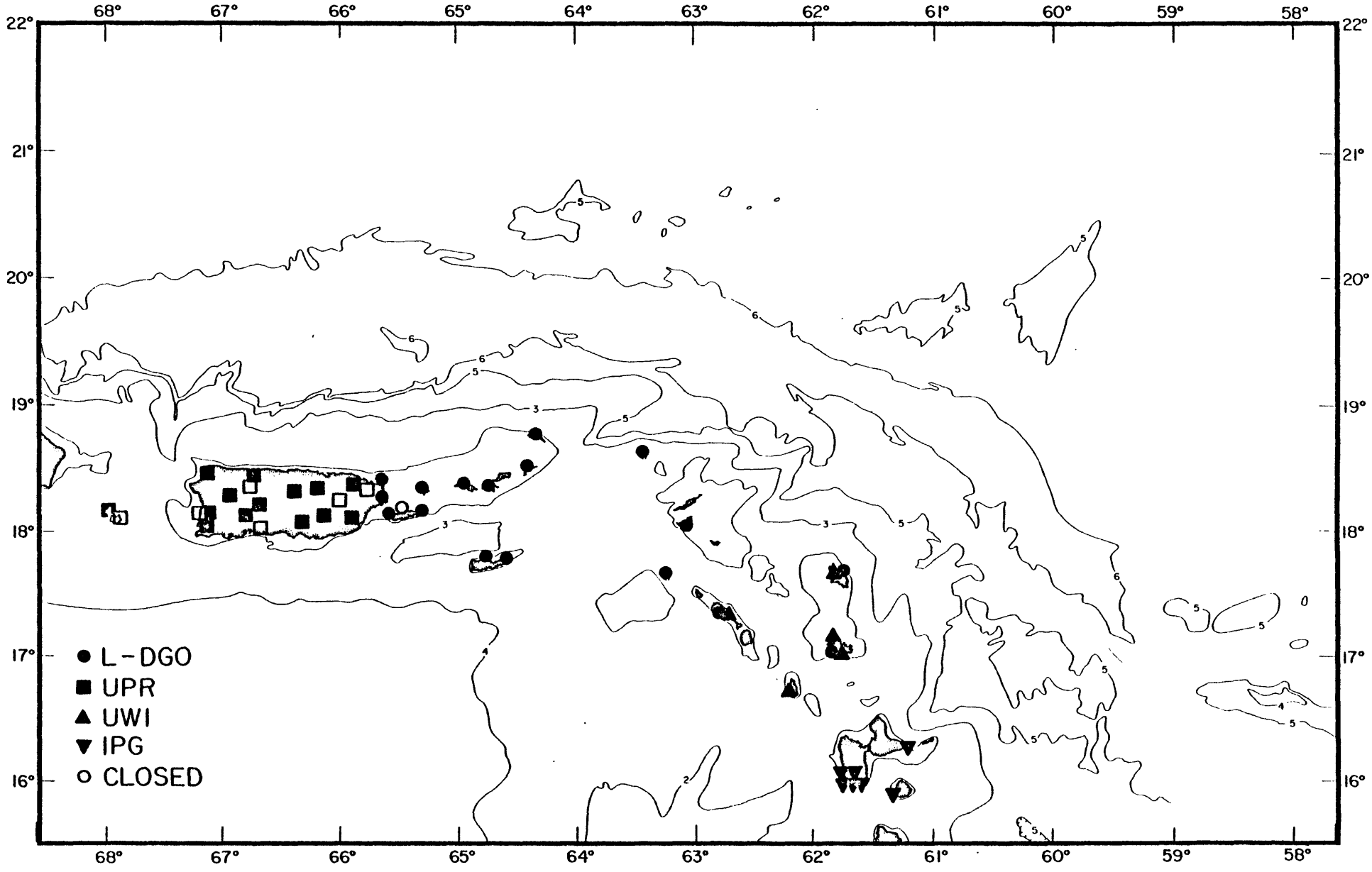

Figure 1b: Seismic stations in the northeastern Caribbean. L-DGO and University of Puerto Rico (UPR) networks began operation in 1975. Note how the L-DGO network completes coverage between the UPR network and the older networks in the northern Lesser Antilles. Bathymetry in kilometers.

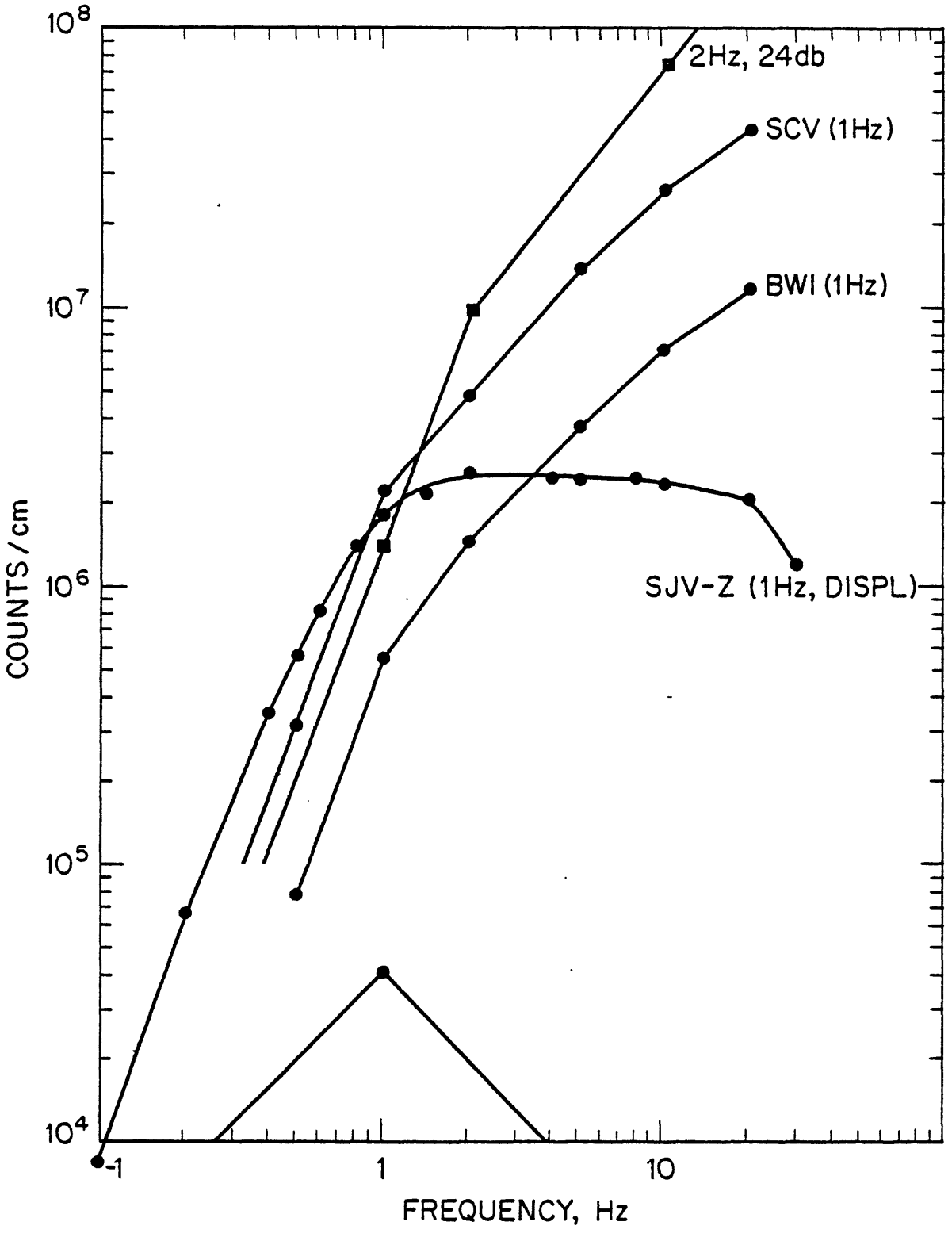

Figure 1c: Response curves for typical stations in the L-DGO network. Most stations now have responses similar to SCV or BWI. The SJV response is an experimental station. The lower curve is the response of the broadband system at St. Thomas.

Table 1

Stations of the Northeastern Caribbean Network

LOCATION	CODE	LAT(N)	LONG(W)	INSTALLATION	GAIN(db)
Anegada British Virgin Island	ABV	18.732	64.337	July 1975	60
Antigua West Indies	AWI	17.045	61.860	Jan 1977	66
Barbuda West Indies	BWI	17.665	61.790	Jan 1977	66
Cotton Garden Point ST. Croix, U.S.V.I.	CGP	17.764	64.584	Sept 1978	66
Camp Garcia Vieques,Puerto Rico	CGV	18.132	65.317	March 1978	66
Cape San Juan Puerto Rico	CSJ	18.383	65.618	April 1975	66
Culebra Culebra, Puerto Rico	CUP	18.335	65.308	July 1975	60
Virgin Gorda British Virgin Island	GPV	18.492	64.404	April 1979	66
Mount Pirata Vieques, Puerto Rico	MTP	18.094	65.557	April 1975	60
Barrio Florida Vieques, Puerto Rico	PWP	18.135	65.455	Apr 75-Mar 78	**
Roosevelt Roads Puerto Rico	RRD	18.236	65.618	April 1975	66
Saba Netherland Antilles	SAB	17.637	63.235	Nov 76-Dec 79	**
Saba Netherland Antilles	SBN	17.621	63.221	Dec 1979	60
St. Croix U.S. Virgin Island	SCV	17.782	64.789	April 1975	66
St. John U.S. Virgin Island	SJV	18.345	64.762	April 1975	66
St. Maarten Antilles	STM	18.012	63.060	Nov 1976	66
St. Christopher West Indies	STK	17.380	62.827	Jan 77-Nov 79	**
St. Christopher West Indies	SKB	17.341	62.840	Nov 1979	60
Sombero West Indies	SWI	18.598	63.426	Nov 1976	60
St. Thomas U.S. Virgin Island	VST	18.354	64.957	April 1975	60

Each station contains a vertical HS-10 Geophone

The following stations also contain two horizontal components:

CUP MTP SJV ABV VST CGP

sites SBN and SKB were installed on Saba and St. Kitts respectively. These stations replaced SAB and STK which were not very sensitive and, therefore, inferior sites.

Besides these changes in station locations, the number of components at the stations in the Virgin Islands has also varied over the three year period. In November 1978 horizontal components were added to all up-island stations. Down-island sites could not have components added because of the limitations on the capacity of the repeater-transmitter at Saba. In April 1980, several of the horizontal instruments were moved to other sites thus creating a wide distribution of high sensitivity, 3-component stations and also several single component sites.

In addition to these refinements in the distribution of our instrumentation, three strong motion accelerographs were installed in the Virgin Islands (Table 2). The present configuration of the network is shown in Figure 1a. Typical response curves for the network stations are shown in Figure 1c, and station calibration data are given in Table 3.

SIGNIFICANT SCIENTIFIC OBSERVATIONS AND RESULTS

1) Focal Mechanisms

The northeastern boundary of the Caribbean plate is a zone of transition between typical island arc subduction in the Lesser Antilles and transform fault type motion in the Cayman trough region.

Strong Motion Accelerographs in the Northeastern Caribbean

Caribbean area

stations:

Anegada	ABV
Antigua	AWI
Barbuda	BWI
St. John	SJV
St. Thomas	VST

ABV
station: Anegada
coordinates: 18 43.92'N Ø64 2Ø.22'W
elevation: 9 ft
site: installed in 55 gal drum on concrete foundation of abandoned building
type of instrument: Kinemetrics SMA-1 1/2g unit
date installed: 3/2Ø/78
serial no.: 3176 (3/2Ø/78)
orinetation: NØ9ØE
sensitivity: N9ØE 1.81cm/Ø.5g UP 2.Ø4cm/Ø.5g NØØØ 1.84cm/Ø.5g
natural freq.: 18.5 hz 17.9 hz 18.3 hz
damping: Ø.6Ø Ø.6Ø Ø.6Ø
records: none
comments: solar cell powered
file updated: 1/18/81 jm

AWI
station: Antigua
coordinates: 17 2.7Ø'N Ø61 51.6Ø'W
elevation: 1113 ft
site: installed in cement cable vault
type of instrument: Kinemetrics SMA-1 1/2g unit
date installed: 2/2Ø/81
serial no.: 961 (2/2Ø/81)
orientation: ØØØN
sensitivity: ØØØN 1.9Øcm/Ø.5g UP 2.Ø3cm/Ø.5g N27Øw 1.9Øcm/Ø.5g
natural freq.: 17.9 hz 17.6 hz 17.8 hz
damping: Ø.6Ø Ø.6Ø Ø.6Ø
records: none
comments: runs off internal batteries
file updated: 4/7/81 jm

BWI
station: Barbuda
coordinates: 17 39.9Ø'N Ø61 47.4Ø'W
elevation: 1Ø8 ft
site: installed in 55 gal. drum cemented in ground
type of instrument: Kinemetrics SMA-1 1/2g unit
date installed: 2/18/81
serial no.: 966 (2/18/81)
orientation: NØØØ
sensitivity: NØØØ 1.91cm/Ø.5g UP 1.74cm/Ø.5g N27ØW 2.Ø8cm/Ø.5g
natural freq.: 17.4 hz 18.6 hz 17.1 hz
damping: Ø.6Ø Ø.6Ø Ø.6Ø
records: none
comments: runs off internal batteries
file updated: 4/7/81 jm

Table 2 (cont'd)

SJV
station: St. John
coordinates: 18 2Ø.7Ø'N Ø64 45.72'W
elevation: 84Ø ft
site: installed on concrete basement of park ranger's house
type of instrument: Kinemetrics SMA-1 1/2g unit
date installed: 3/22/78
serial no.: 317Ø (3/22/78)
orientation: N27ØW

sensitivity:	N27ØW 1.72cm/Ø.5g	UP 1.82cm/Ø.5g	N18Ø 1.67cm/Ø.5g
natural freq.:	18.5 hz	18.1 hz	19.Ø hz
damping:	Ø.6Ø	Ø.6Ø	Ø.6Ø

records: none
comments: runs off trickle charger
file updated: 1/18/81 jm

VST
station: St. Thomas
coordinates: 18 21.24'N Ø64 57.42'W
elevation: 1116 ft
site: installed on concrete pier in vault
type of instrument: Kinemetrics SMA-1 1/2g unit
date installed: 9/?/79
serial no.: 962 (3/5/81)
orientation: NØØØ

sensitivity:	NØØØ 1.97cm/Ø.5g	UP 1.95cm/Ø.5g	N27ØW 1.89cm/Ø.5g
natural freq.:	17.2 hz	17.4 hz	18.9 hz
damping:	Ø.6Ø	Ø.6Ø	Ø.6Ø

records: 2/14/8Ø
comments: runs off trickle charger
prior to 9/?/79 there was another SMA here
from 9/?/79 to 3/5/81 #1Ø64 was here at same orientation
file updated: 4/7/81 jm

Table 3

NORTHEASTERN CARIBBEAN SEISMIC NETWORK
NOMINAL VALUES OF STATION GAIN

Component	Station	Seismo Type	Coil Resistance	Nat Freq	Damping	Counts/cm at 10 Hz
1	MTP Z	HS-10	50 K	1 Hz	.7	7×10^6
2	N	HS-10	4 K	1 Hz	.7	1×10^7
3	E	HS-10	4 K	1 Hz	.7	1×10^7
4	CUP Z	HS-10	50 K	1 Hz	.7	7×10^6
5	N	HS-10	4 K	1 Hz	.7	1×10^7
6	E	HS-10	4 K	1 Hz	.7	1×10^7
7	SJV Z	HS-10	50 K	1 Hz	.7	2.4×10^6
8	N	HS-10	4 K	1 Hz	.7	1.8×10^6
9	E	HS-10	4 K	1 Hz	.7	1.8×10^6
10	CGP Z	HS-10	50 K	1 HZ	.7	7×10^6
11	N	HS-10	4 K	1 HZ	.7	1×10^7
12	E	HS-10	4 K	1 HZ	.7	1×10^7
13	ABV Z	HS-10	50 K	1 HZ	.7	1×10^6
14	N	HS-10	4 K	1 HZ	.7	1×10^7
15	E	HS-10	4 K	1 HZ	.7	1×10^7
16	CSJ	HS-10	50 K	1 HZ	.7	2.8×10^7
17	RRD	HS-10	50 K	1 HZ	.7	2.8×10^7
18	CGV	HS-10	50 K	1 HZ	.7	2.8×10^7
19	SCV	HS-10	50 K	1 HZ	.7	2.8×10^7
20	GPV	HS-10	4 K	1 HZ	.7	4×10^7
21	SWI	HS-10	50 K	1 HZ	.7	7×10^6
22	SBN	HS-10	4 K	2 HZ	.7	4×10^7
23	STM	HS-10	4 K	2 HZ	.7	4×10^7
24	SKB	HS-10	50 K	1 HZ	.7	7×10^6
25	AWI	HS-10	4 K	2 HZ	.7	4×10^7
26	BWI	HS-10	50 K	1 HZ	.7	7×10^6
27	VST Z	HS-10	4 K	1 HZ	.7	7×10^6
28	VST N	HS-10	4 K	1 HZ	.7	7×10^6
29	VST E	HS-10	4 K	1 HZ	.7	7×10^6
30	VST Z (bb)	HS-10	4 K	1 HZ	.7	$\frac{1 \text{ HZ}}{4.1 \times 10^4}$,
31	VST N (bb)	HS-10	4 K	1 HZ	.7	$\frac{1 \text{ HZ}}{4.5 \times 10^4}$,
32	VST E (bb)	HS-10	4 K	1 HZ	.7	$\frac{1 \text{ HZ}}{3.4 \times 10^4}$,

NOTE: CUP, SJV, CGV, GPV, STM and AWI are trigger stations. SJV has a displacement response. VST recorded on channels 30, 31 and 32 is a broadband response.

The tectonic deformation along this boundary is characterized by some complex combination of subduction and oblique subduction processes. The details of this deformation, however, are not yet understood, and additional focal mechanism data are required to understand more completely the tectonic processes in this region.

During the period covered by this report focal mechanisms of four earthquakes which occurred in the northeastern Caribbean have been determined using body wave first motion data from the WWSSN (Figure 2). These results combined with the focal mechanism results of Molnar and Sykes (1969), Rial (1978), Kafka and Weidner (1979), and McCann et al. (1981) are shown in a map view in Figure 3. The results shown in Figure 3 indicate that a wide variety of styles of seismotectonic deformation is presently occurring in the northeastern Caribbean, and no simple model of relative plate motion is apparent. Events 12, 23, 109, 110 are low angle thrust faulting earthquakes associated with the Lesser Antilles subduction zone and are typical of shallow seismic activity seaward of an island arc. For event 22 the N-NW striking nodal plane is well constrained. The second nodal plane is poorly constrained, however, and can be rotated to produce a greater component of normal faulting without severely violating the P wave data. This event can be interpreted as resulting from extensional stresses normal to and seaward of the Lesser Antilles island arc as is typical of other subduction zones. Thus, focal mechanisms in the southern portion of the Lesser Antilles are consistent with a simple model of the North American plate subducting beneath the Caribbean plate.

Figure 2a

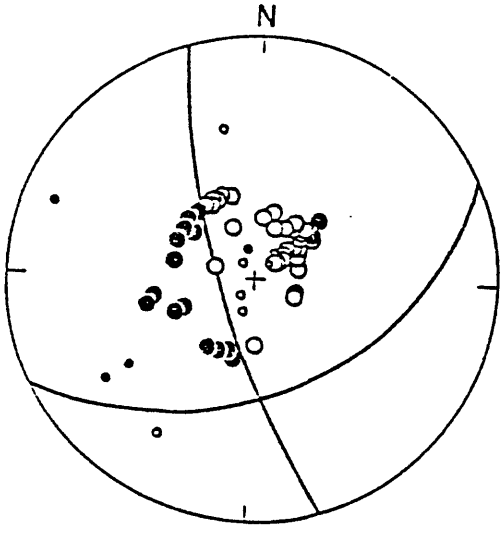

25 DEC. 1969
event 22; m_b = 6.4

Figure 2b

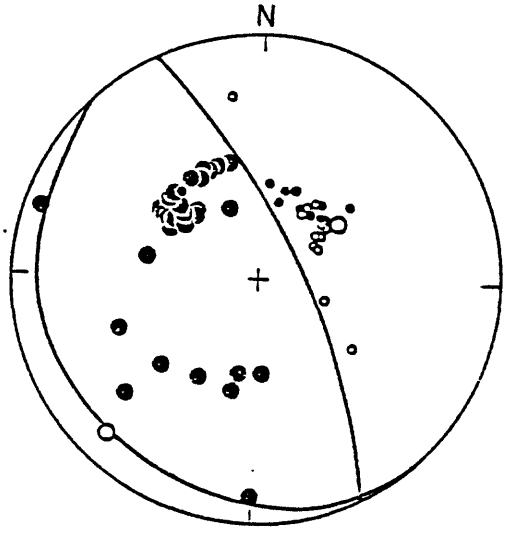

15 MAY 1969
event 23; m_b = 5.7

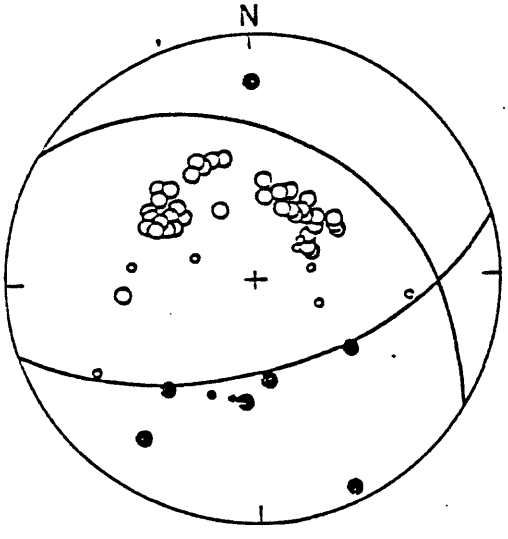

8 JULY 1970
event 24; m_b = 5.8

Figure 2c

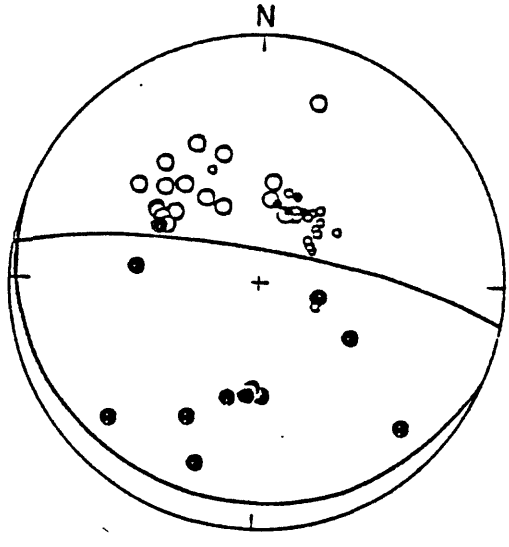

2 MAY 1968
event 25; m_b = 5.6

Figure 2d

Figure 2: P-wave first motion data and focal mechanism results for (a) event 22, (b) event 23, (c) event 24, and (d) event 25. Open circles represent dilatation and solid circles represent compression. Larger symbols indicate good to excellent readings and smaller symbols represent average to poor readings. Data are projected on a lower focal hemisphere.

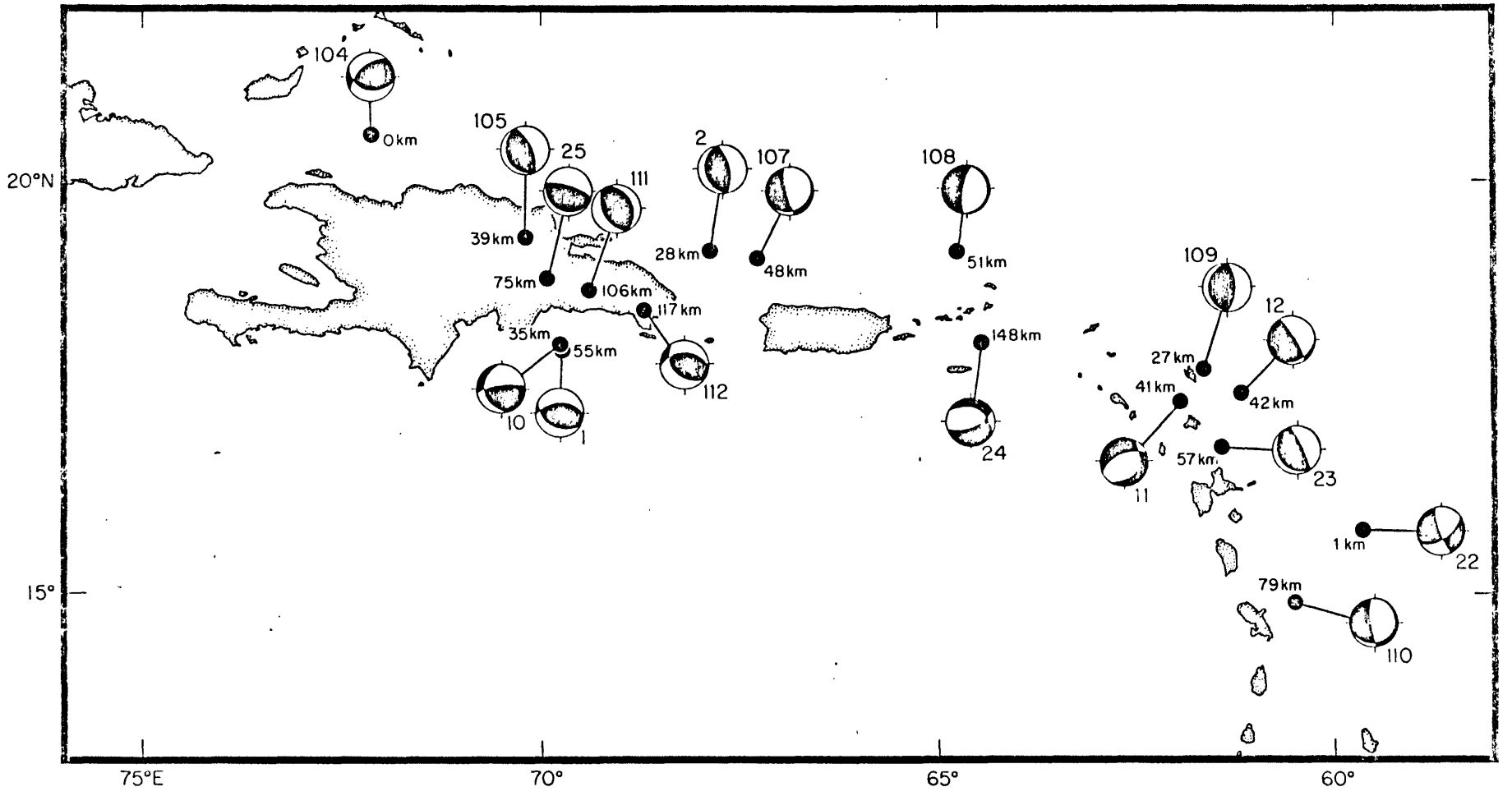

Figure 3: Focal mechanism results for events shown in Figure 2 along with results of other studies. Events 1 and 2 are from Kafka and Weidner (1979). Events 10 and 12 are from Rial (1978). Events 104, 105, and 107-112 are from Molnar and Sykes (1969), and event 11 is from McCann et al. (1981). Lower focal hemispheres are used throughout, and dark areas represent compressional quadrants.

As the northern end of the Lesser Antilles arc is approached, however, several deviations from a simple subduction model are observed. Event 11 in Figure 3, for example, is a shallow normal faulting event and is not typical of island arc regions. McCann et al. (1981) argue that the tensional stresses parallel to the trend of the island arc inferred from this focal mechanism are a result of perturbations in the stress field caused by the subduction of the Barracuda ridge (see below). Northwest of event 11 a relatively low level of seismic activity is observed between 62°W and 64°W both in the teleseismic data (Figure 4a) and the local network data (Figure 4b). To the west of 64°W the descending slab dips to the south (Figure 5) as compared to the westward dip of the slab in the Lesser Antilles. Also, earthquake focal mechanisms to the west of 64°W deviate significantly from that which would be expected for a simple model of a subduction zone. This southerly dip of the slab near Puerto Rico and the Virgin Islands and the predominance of thrust faulting earthquakes with large components of slip in a southerly direction in the Hispaniola region (Figure 3) suggests a component of N-S motion between the Caribbean and North American plates.

Event 108 occurred to the north of the Virgin Islands before the installation of the Lamont-Doherty seismic network. A relatively high level of seismicity is observed both in the teleseismic data (Figure 4a) and the local network data (FIgure 4b) in the region near event 108, and the details of the subduction process between 64°W and 66°W has been of major concern in our research. An event of m_b = 5.2 (January 22, 1979) was recorded by the Lamont-Doherty network and

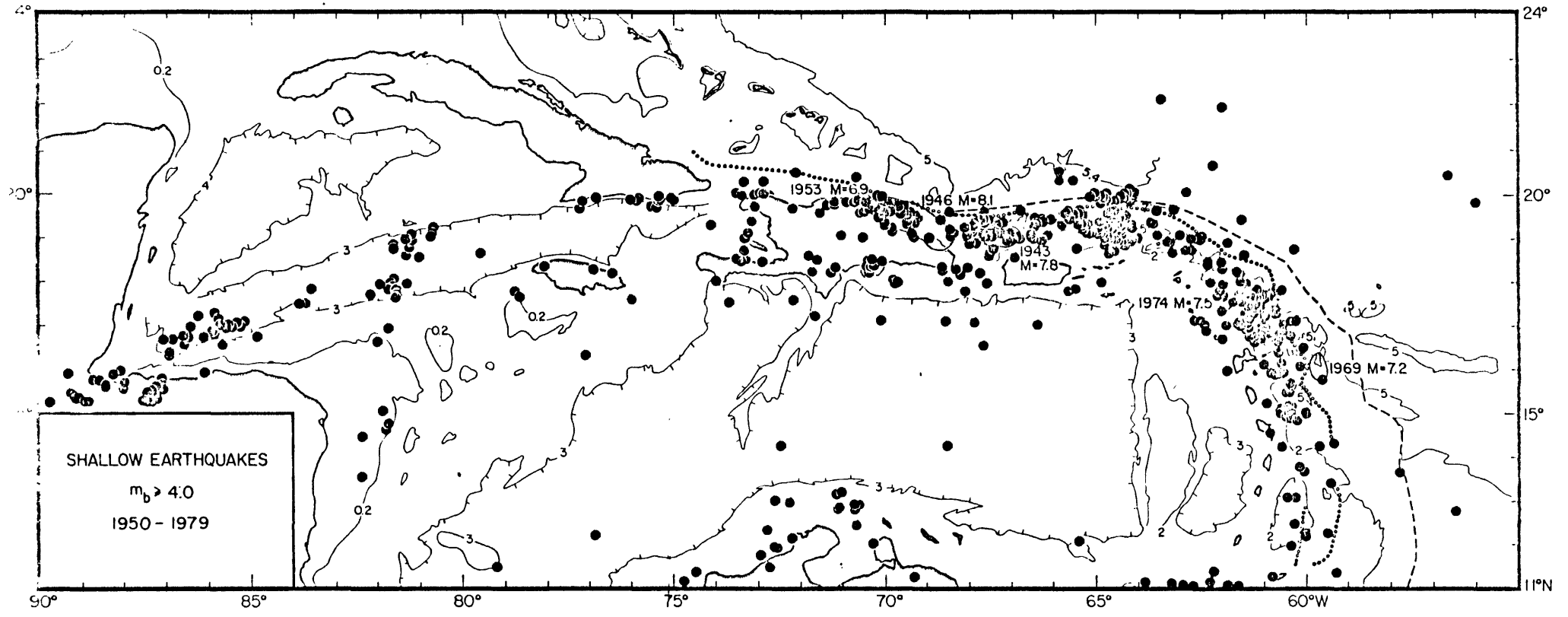

Figure 4a: Shallow earthquakes, 1950-1959, as located by computer. Note two large clusters of earthquakes in the northeast portion of the seismic zone (from Sykes and McCann, 1981).

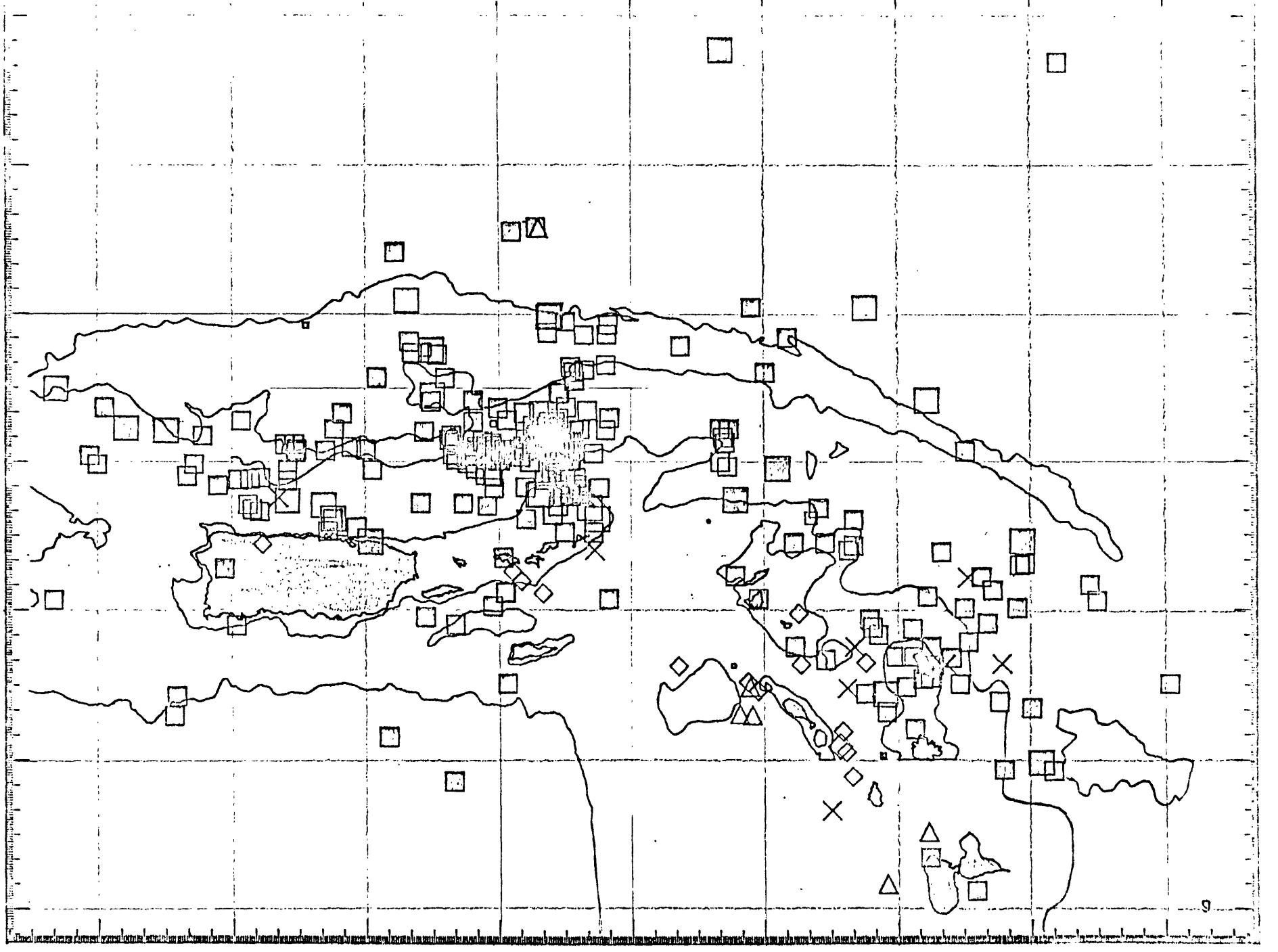

Figure 4b: Events $m_b \geq 3.0$ located by local networks for the years 1977-1980. Note clustering near 19°N, 65°W and 18°N, 62°W where bathymetric features intersect the trends.

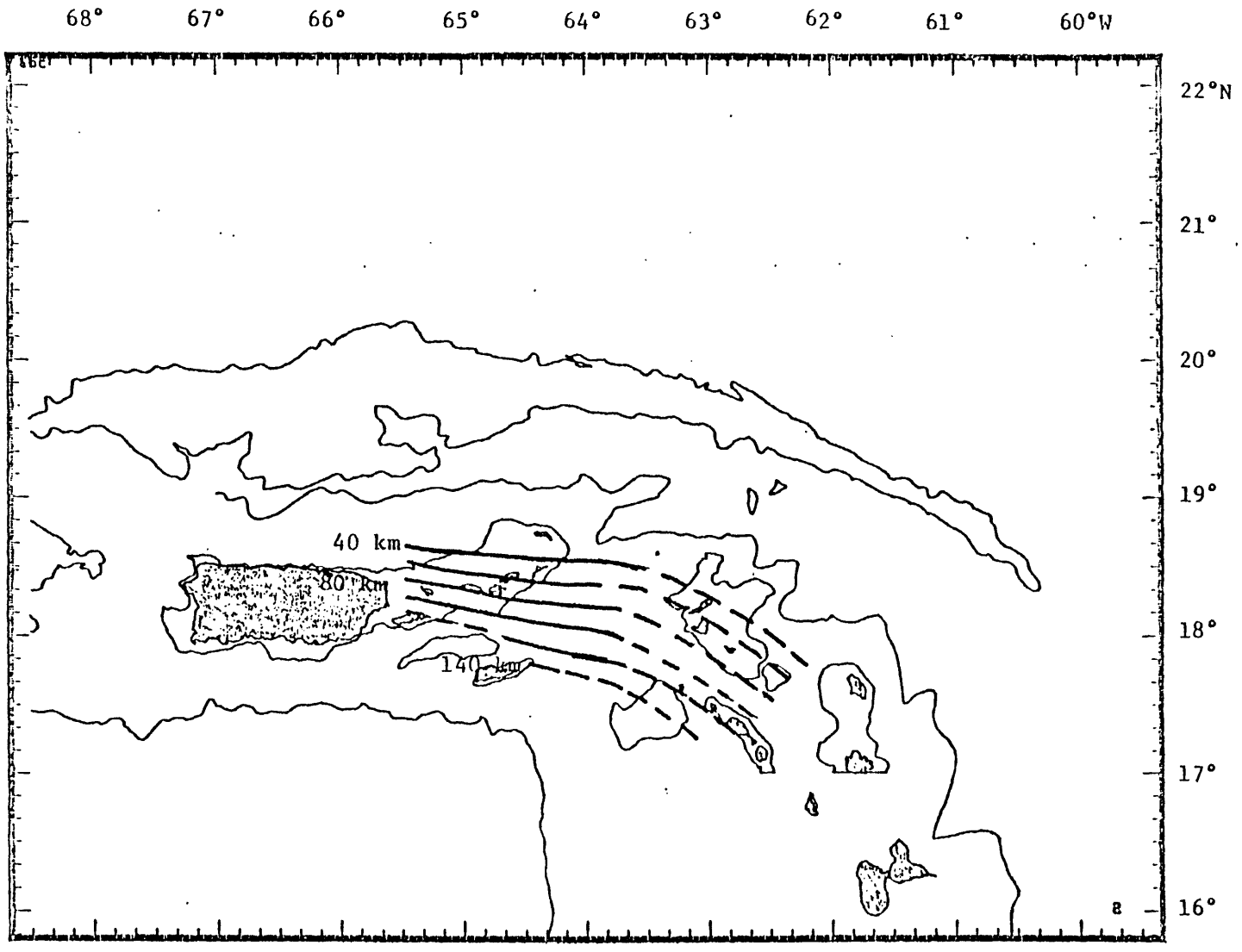

Figure 5: Contours of depth to top of seismic zone for the northeast Caribbean. Contours are drawn using events located by L-DGO seismic network. The data indicate that the subducted portion of the North American plate is continuous and changes from a westerly dipping structure beneath the Lesser Antilles to southerly dipping beneath Puerto Rico.

locates within ten kilometers of event 108. By combining the first motion data from the network and teleseismically recorded body and surface wave data, the focal mechanism and depth of the 1979 event can be determined and the focal mechanism and depth of event 108 can be more tightly constrained. We have already begun the surface wave analysis for this pair of events, and we have found that extremely coherent surface wave spectra have been recorded. Thus, we expect to obtain very well constrained solutions for these two events.

Event 24 is located ∿100 km to the south of event 108, and the ISC reports a depth of 148 km for this event. Figure 5 shows that the seismic zone dips to a depth of ∿100 km in the epicentral region of event 24 and accurate depth determination for this event may yield important constraints on the stress field within the descending slab in this region. The focal mechanism of this event is neither consistent with down dip compression nor down dip tension in the subducted lithosphere and the relationship between the stress field in the slab and the tectonic processes in this region requires further investigations.

2) Tectonics and Seismicity

The microearthquakes along the northeastern margin of the Caribbean plate are not evenly distributed along the main seismic zone. Most shocks of magnitude 3 or greater are confined to limited portions of the inner wall of the Puerto Rico trench (Figure 4a,b). These seismically active regions are also identified as topographically high

portions of the inner wall. Magnetic lineations, topographic trends and sites of uplift indicate that two clusters of seismic activity on the inner wall of the trench may lie near parts of a large fracture zone (i.e., the Barracuda ridge) that has been overridden by the northeast corner of the Caribbean plate. Figure 6 shows the recent tectonic framework of the northeastern Caribbean. Over the last few million years plate motions have carried the Barracuda ridge, shown as wavy lines, into the subduction zone of the northern Lesser Antilles. The interaction of this ridge with the arc has deformed the sediments on the inner wall of the trench, uplifted the frontal arc, and dramatically increased the seismicity in the vicinity of the interaction. Murphy and McCann (1979) noted the clustering of micro-earthquakes north of the Virgin Islands. They also noted that these shocks lie near the Main ridge (Figure 6); it truncates well defined accretionary structures on the inner wall and stands some 1.5 km above the surrounding seafloor. This ridge is now believed to be the north-western extension of the Barracuda ridge.

McCann et al. (1981) identified a seismically active segment of the northern Lesser Antilles. This region, 16.5 to 18.0°N, which lies in the zone of interaction with the Barracuda ridge, was the site of a large intraplate earthquake of the normal faulting type (Figure 3, event 11; Figure 4a). The fault plane as defined by locally recorded aftershocks strikes N20 to N35 and dips some 45° to the southeast. It is likely that this shock is related to tectonic movements associated with the subduction of the Barracuda ridge.

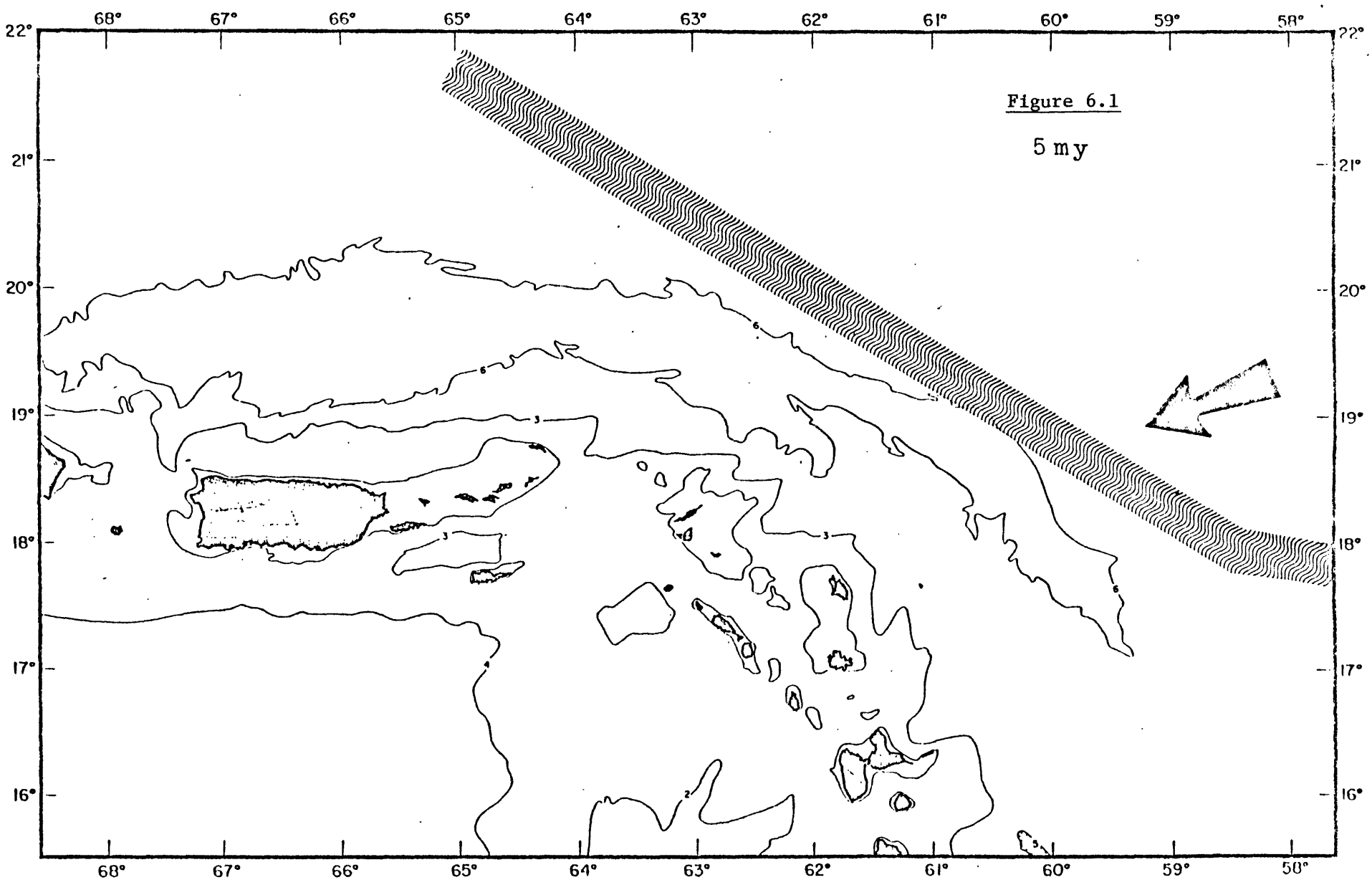

Figure 6: Postulated history of the interaction between the Caribbean plate and Barracuda rige. 6.1, 6.2, and 6.3 show position of ridge (wavy lines) at 5.0 and 2.4 million years BP and its inferred position today. 6.4 shows the main tectonic elements in the region; solid line is position of southeastern flank of the Barracuda ridge (BR). Main ridge (MR) is extension that has yet to be subducted. Regions of uplift are shown by stippling. Hatching is region where sediments on the inner wall of the trench have been deformed by the passage of the ridge. Perched basins (PB) are old accretionary structures not yet affected by the ridge.

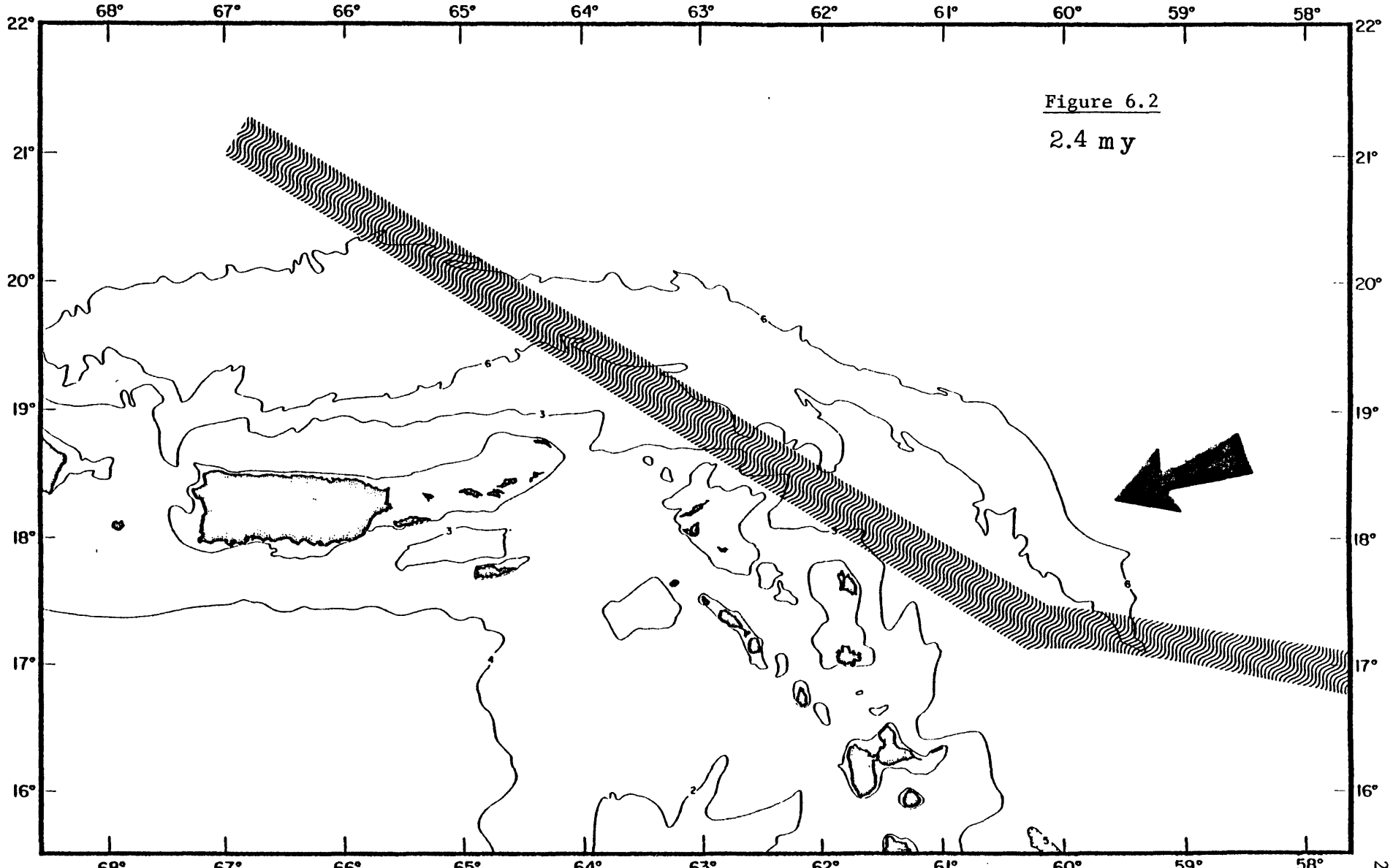

Figure 6.2

2.4 m y

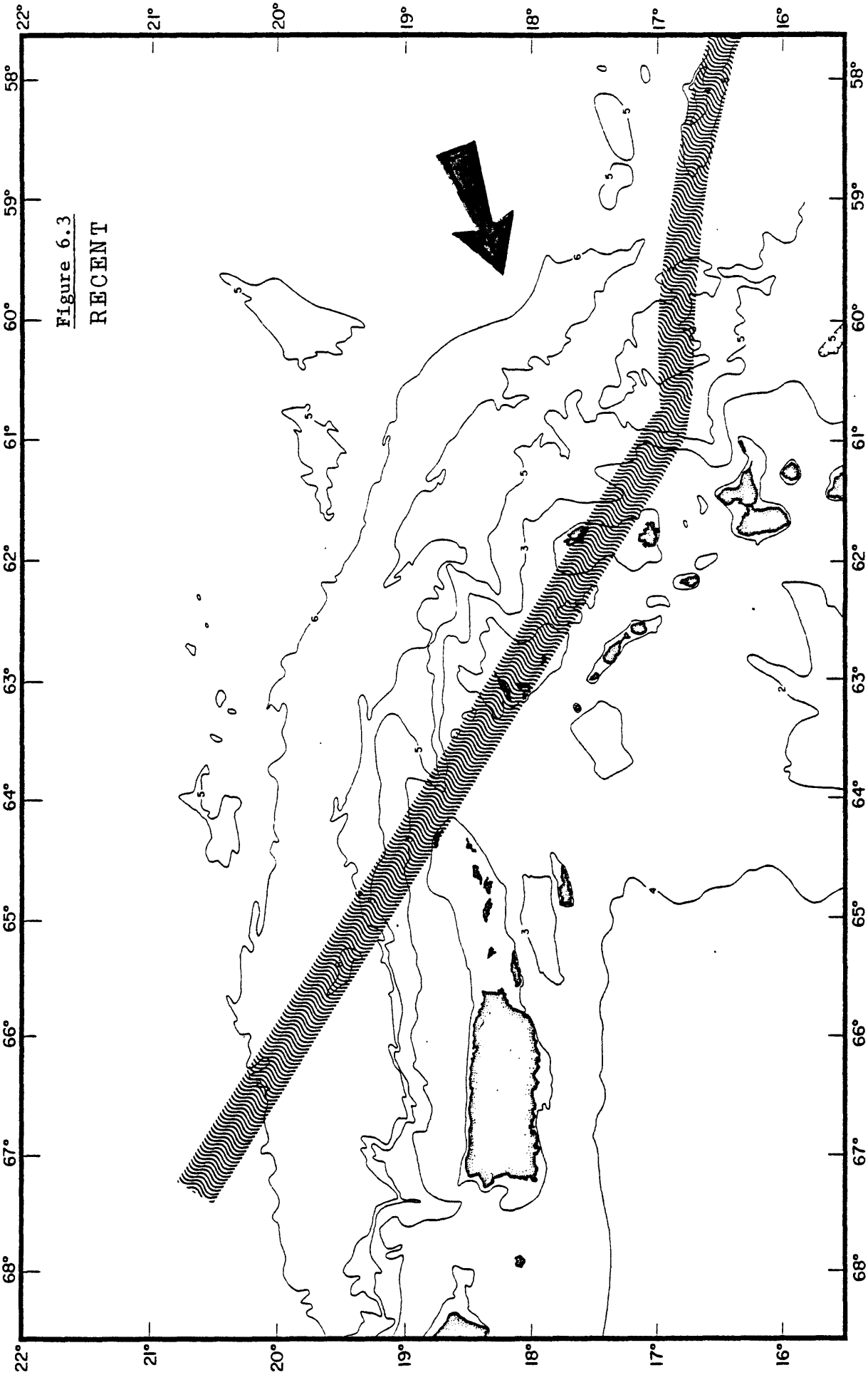

Figure 6.3

RECENT

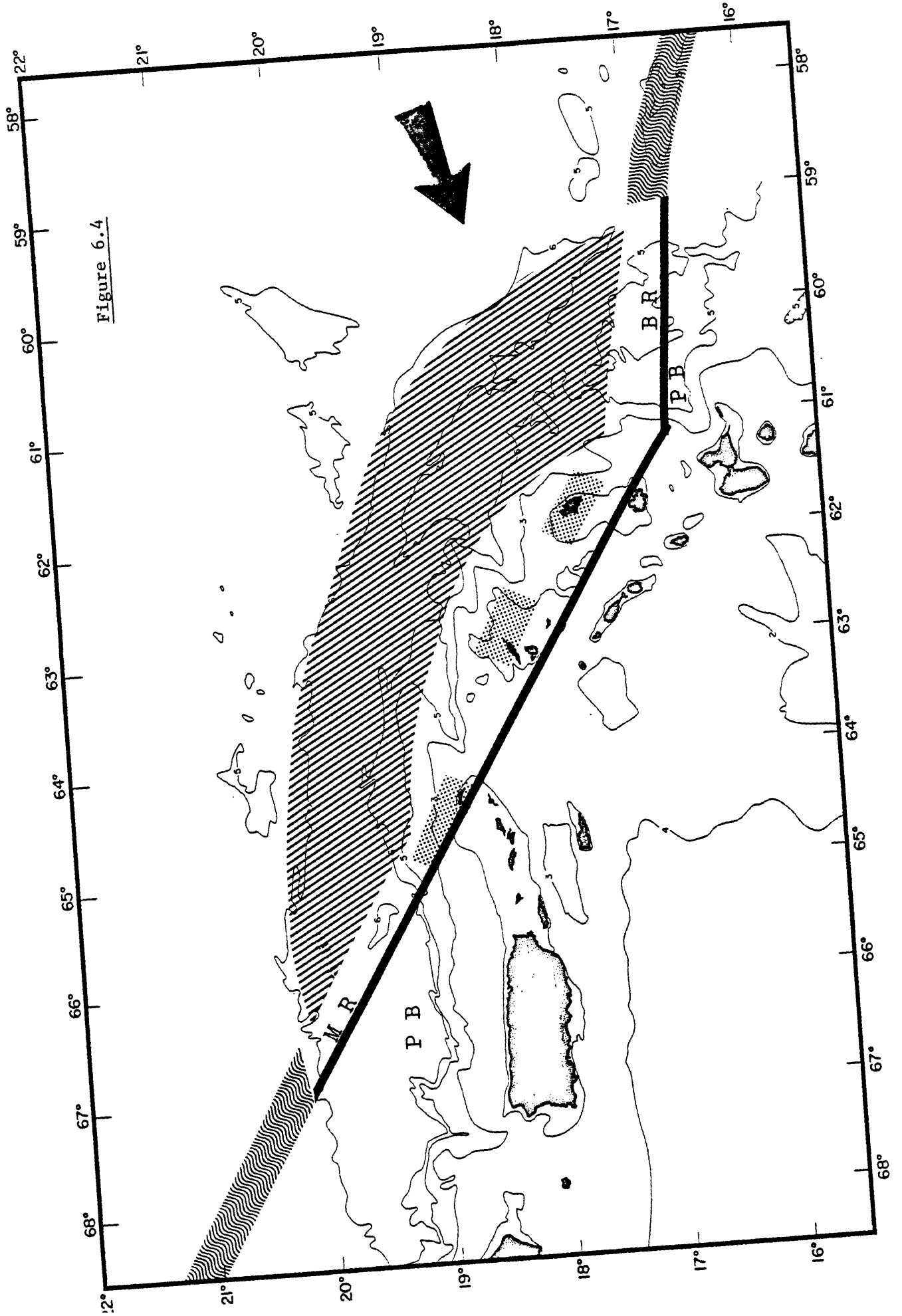

Figure 6.4

There appears to be a dichotomy in the mode of seismic energy release between the up-island and down-island clusters of seismicity. Whereas, the down-island cluster is characterized by main shock - aftershock sequences, the up-island cluster is characterized by swarms. To date no swarms have been observed in the subduction zone of the northern Lesser Antilles. Numerous swarms have been observed, however, north of the Virgin Islands. These swarms are primarily concentrated in the region where the Main ridge interacts with the crustal portion of the Caribbean plate (Figure 6), and they are not evenly distributed in time. A typical surge in the seismic activity north of the Virgin Islands is characterized by the occurrence of a swarm followed by at least one additional swarm within a few tens of days and not more than about 40 km from the initial swarm. This type of sequence is very common when the swarms contain earthquakes of magnitude 4.0 or greater.

A first approximation of the structure of the subducted North American plate in the Virgin Islands and the northernmost Lesser Antilles has been obtained. The contours shown in Figure 5 have been obtained by compiling all microearthquakes with standard errors in epicenter and depth of less than 10 km occurring during the period 1977-1979. The upper surface of the seismic zone associated with the subducted plate has been determined along various vertical cross-sections, and isobaths of this upper surface have been contoured as shown in Figure 5.

3) Analysis of Digital Seismograms

The digital seismograms collected by the Caribbean network are being used to study the source parameters of earthquakes in the area and the attenuation of seismic radiation. In one investigation, the seismic moments and stress drops of 23 earthquakes ($1.1 \leq M \leq 2.4$) that occurred during a swarm in the Anegada passage were determined from the analysis of the P-waveforms. The simple waveforms of these events allowed us to use time domain measurements of displacement pulse width and area to estimate the fault radius and seismic moment, respectively, for each earthquake. The digital data also enabled us to determine arrival times of body waves with the precision necessary to resolve the spatial extent of the swarm region. By combining the stress drop data with the hypocentral locations of the swarm events we obtained a detailed picture of the spatial variability of stress drop on a scale of hundreds of meters (Figure 7).

The results of this study show that the static stress drops of the swarm events varied by an order of magnitude (from 0.2 to 2 bars), although the events all occurred within 1 km of each other. The stress drops of these earthquakes systematically increased with their seismic moments. The fault radii of these shocks increased with seismic moment, but only by a factor of 2 for a 100-fold increase in seismic moment. The velocity waveforms of large shocks were more impulsive than those of the smaller events, implying that the dynamic stress drop also increased with seismic moment. We are studying other

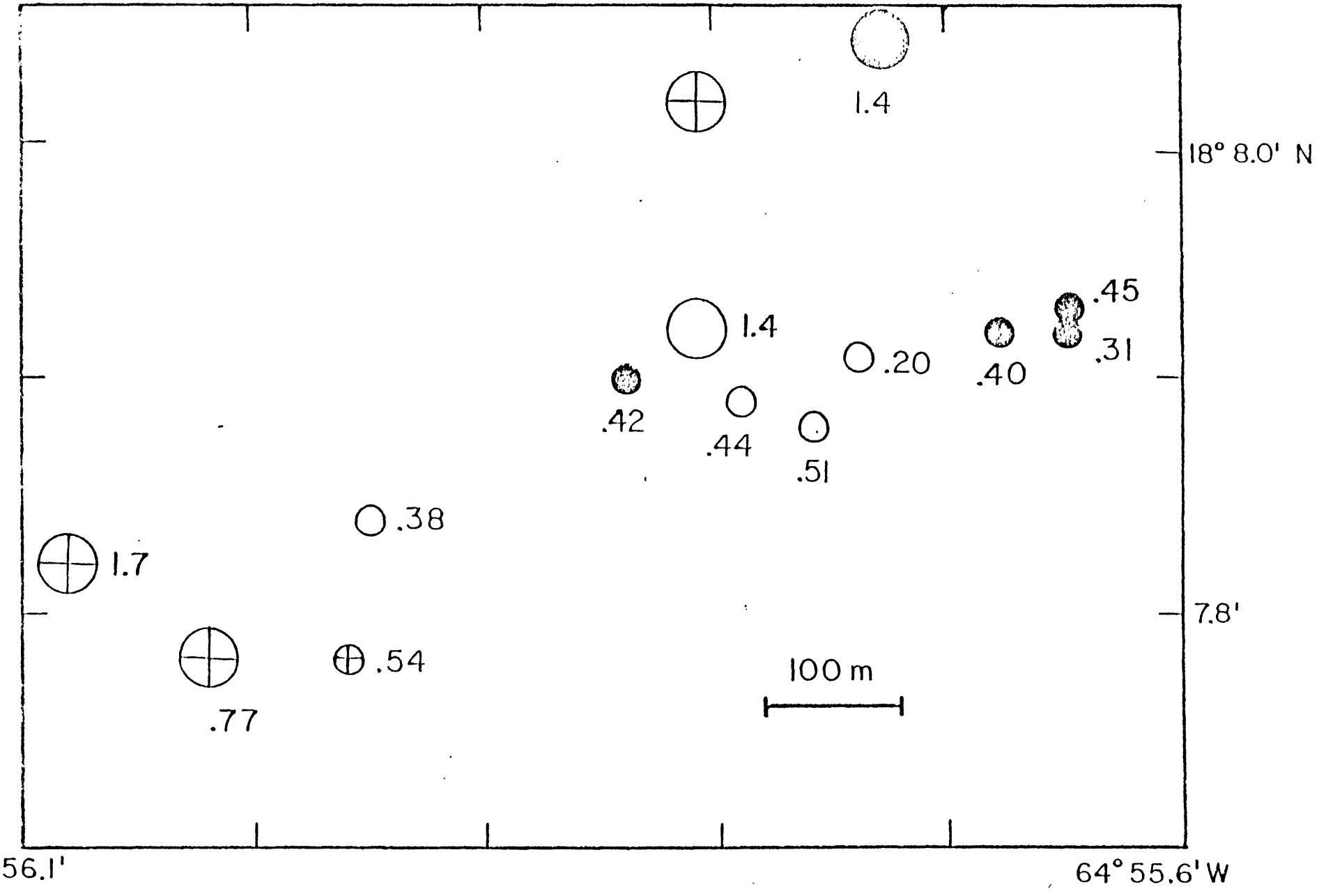

Figure 7: Detailed map of the epicenters of some of the swarm events as obtained through the joint location procedure. The static stress drops of the events are indicated by the numbers next to the symbols. The larger symbols represent the events greater than magnitude 2.

earthquake sequences to determine how common this relationship between stress drop and seismic moment is for earthquakes between magnitude 1 and 5.

The spectral fall-off of earthquakes in the region were used to estimate seismic attenuation. Events farther away from a given station are observed to be depleted in high frequency energy. By plotting spectral fall-offs of twenty shallow events as a function of travel time of their seismic waves, we obtained a Q for P-waves of 390 ± 30 and a Q for S-waves of 670 ± 70. These values of Q are valid over the frequency range of 10 to 30 hertz. It is notable that, for these frequencies, Q_s exceeds Q_p. This observation implies that the attenuation mechanism that operates at these high frequencies differs from the mechanism at longer periods were $Q_p < Q_s$. Earthquakes that occurred at depths of about 100 km contained a relatively large amount of high-frequency energy compared with shallow events at comparable distances from the receiver. We interpret this as a manifestation of increasing Q with depth, rather than a difference in source parameter.